

## SOFT MODES, QUANTUM TRANSPORT AND KINETIC ENTROPY<sup>§</sup>

YU. B. IVANOV<sup>†</sup>, J. KNOLL, H. VAN HEES, D. N. VOSKRESENSKY<sup>‡</sup>  
*Gesellschaft für Schwerionenforschung mbH, Planckstr. 1, 64291 Darmstadt, Germany*  
*E-mail: Y.Ivanov@gsi.de, J.Knoll@gsi.de, D.Voskresensky@gsi.de*

The effects of the propagation of particles which have a finite life-time and an according width in their mass spectrum are discussed in the context of transport descriptions. In the first part the coupling of soft photon modes to a source of charged particles is studied in a classical model which can be solved completely in analytical terms. The solution corresponds to a re-summation of certain field theory diagrams. The general properties of broad resonances in dense finite temperature systems are discussed at the example of the  $\rho$ -meson in hadronic matter. The second part addresses the problem of transport descriptions which also account for the damping width of the particles. The Kadanoff–Baym equation after gradient approximation together with the  $\Phi$ -derivable method of Baym provides a self-consistent and conserving scheme. Memory effects appearing in collision term diagrams of higher order are discussed. We derive a generalized expression for the nonequilibrium kinetic entropy flow, which includes corrections from fluctuations and mass-width effects. In special cases an  $H$ -theorem is proved. Memory effects in collision terms provide contributions to the kinetic entropy flow that in the Fermi-liquid case recover the famous bosonic type  $T^3 \ln T$  correction to the specific heat of liquid Helium-3.

With the aim to describe the collision of two nuclei at intermediate or even high energies one is confronted with the fact that the dynamics has to include particles like the delta or rho-meson resonances with life-times of less than 2 fm/c or equivalently with damping widths above 100 MeV. Also the collisional damping rates deduced from presently used transport codes are of the same order, whereas typical mean temperatures range between 50 to 150 MeV depending on beam energy. Thus, the damping width of most of the constituents in the system can by no means be treated as a perturbation. As a consequence the mass spectrum of the particles in the dense matter is no longer a sharp delta function but rather acquires a width due to collisions and decays. One thus comes to a picture which unifies *resonances* which have

---

<sup>§</sup>Combined contribution summarizing the talks of J. Knoll on the subject “Soft Modes and Resonances in Dense Matter” and Y.B. Ivanov on the subject “Quantum Transport and Kinetic Entropy”.

<sup>†</sup>Permanent address: Kurchatov Institute, Kurchatov sq. 1, Moscow 123182, Russia

<sup>‡</sup>Permanent address: Moscow Institute for Physics and Engineering, Kashirskoe sh. 31, Moscow 115409, Russia

already a width in vacuum due to decay modes with the "states" of particles in dense matter, which obtain a width due to collisions (collisional broadening).

The theoretical concepts for a proper many body description in terms of a real time nonequilibrium field theory have already been devised by Schwinger<sup>1</sup>, Kadanoff and Baym<sup>2</sup>, and Keldysh<sup>3</sup> in the early sixties, extensions to relativistic plasmas followed by Bezzerides and DuBois<sup>4</sup>. First investigations of the quantum effects on the Boltzmann collision term were given by Danielewicz<sup>5</sup>, the principal conceptual problems on the level of quantum field theory were investigated by Landsmann<sup>6</sup>, while applications which seriously include the finite width of the particles in transport descriptions were carried out only in recent times, e.g. refs. <sup>5,7,8,9,10,11,12,13</sup>. For resonances, e.g. the delta resonance, it was natural to consider broad mass distributions and ad hoc recipes have been invented to include this in transport simulation models. However, many of these recipes are not correct as they violate some basic principles like detailed balance (see discussion in ref. <sup>7</sup>), and the description of resonances in dense matter has to be improved<sup>12</sup>.

In this contribution the consequences of the propagation of particles with short life-times are discussed. First we address a genuine problem related to the occurrence of broad damping width, i.e. the soft mode problem. At the classical level we investigate the coupling of a coherent classical field, the Maxwell field, to a stochastic source described by the Brownian motion of a charged particle. In this case the classical current-current correlation function, can be obtained in closed analytical terms and discussed as a function of the macroscopic transport properties, the friction and diffusion coefficient of the Brownian particle. The result corresponds to a partial re-summation of photon self-energy diagrams in the real-time formulation of field theory. Subsequently the properties of particles with broad damping width is illustrated at the example of the  $\rho$ -meson in dense matter at finite temperature. In the final part we discuss how particles with such broad mass-width can be described consistently within a transport theoretical picture.

We are going to argue that the Kadanoff–Baym equations in the first gradient approximation together with the  $\Phi$ -functional method of Baym<sup>14</sup> provide a proper frame for kinetic description of systems of particles with a broad mass-width. To this end, we discuss relevant problems concerning charge and energy–momentum conservation, thermodynamic consistency, memory effects in the collision term and the growth of entropy in specific cases. For simplicity we concentrate on systems of non-relativistic particles. Generalization to systems of relativistic particles and bosonic mean fields can be straight forwardly done along the lines given in ref. <sup>15</sup>.

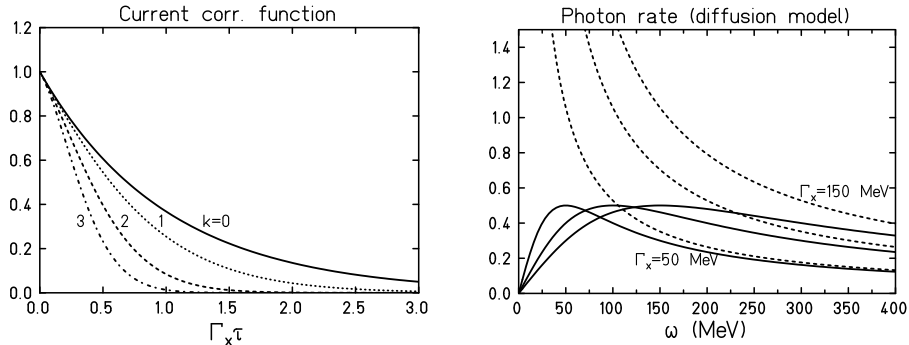


Figure 1: Left: Current-current correlation function in units of  $e^2 \langle v^2 \rangle$  as a function of time (in units of  $1/\Gamma_x$ ) for different values of the photon momentum  $q^2 = 3k^2\Gamma_x^2/\langle v^2 \rangle$  with  $k = 0, 1, 2, 3$ . Right: Rate of real photons  $d^2N/(d\omega dt)$  in units of  $4\pi e^2 \langle v^2 \rangle / 3$  for a non-relativistic source for  $\Gamma_x = 50, 100, 150$  MeV; for comparison the IQF results (dashed lines) are also shown.

## 1 Bremsstrahlung from Classical Sources

For a clarification of the soft mode problem we discuss an example in classical electrodynamics. We consider a stochastic source, the hard matter, where the motion of a single charge is described by a diffusion process in terms of a Fokker-Planck equation for the probability distribution  $f$  of position  $\mathbf{x}$  and velocity  $\mathbf{v}$

$$\frac{\partial}{\partial t} f(\mathbf{x}, \mathbf{v}, t) = \left( D\Gamma_x^2 \frac{\partial^2}{\partial \mathbf{v}^2} + \Gamma_x \frac{\partial}{\partial \mathbf{v}} \mathbf{v} - \mathbf{v} \frac{\partial}{\partial \mathbf{x}} \right) f(\mathbf{x}, \mathbf{v}, t). \quad (1)$$

Fluctuations also evolve in time according to this equation, or equivalently by a random walk process<sup>13</sup>, and this way determine correlations. This charge is coupled to the Maxwell field. On the assumption of a non-relativistic source, this case does not suffer from standard pathologies encountered in hard thermal loop (HTL) problems of QCD, namely the collinear singularities, where  $\mathbf{v}\mathbf{q} \approx 1$ , and from diverging Bose-factors. The advantage of this Abelian example is that damping can be fully included without violating current conservation and gauge invariance. This problem is related to the Landau–Pomeranchuk–Migdal effect of bremsstrahlung in high-energy scattering<sup>16</sup>.

The two macroscopic parameters, the spatial diffusion  $D$  and friction  $\Gamma_x$  coefficients determine the relaxation rates of velocities. In the equilibrium limit ( $t \rightarrow \infty$ ) the distribution attains a Maxwell-Boltzmann velocity distribution with the temperature  $T = m \langle v^2 \rangle / 3 = mD\Gamma_x$ . The correlation function can

be obtained in closed form and one can discuss the resulting time correlations of the current at various values of the spatial photon momentum  $\mathbf{q}$ , Fig. 1 (details are given in ref. <sup>13</sup>). For the transverse part of the correlation tensor this correlation decays exponentially as  $\sim e^{-\Gamma_x \tau}$  at  $\mathbf{q} = 0$ , and its width further decreases with increasing momentum  $q = |\mathbf{q}|$ . The in-medium production rate is given by the time Fourier transform  $\tau \rightarrow \omega$ , Fig. 1 (right part). The hard part of the spectrum behaves as intuitively expected, namely, it is proportional to the microscopic collision rate expressed through  $\Gamma_x$  (cf. below) and thus can be treated perturbatively by incoherent quasi-free (IQF) scattering prescriptions. However, independently of  $\Gamma_x$  the rate saturates at a value of  $\sim 1/2$  in these units around  $\omega \sim \Gamma_x$ , and the soft part shows the inverse behavior. That is, with increasing collision rate the production rate is more and more suppressed! This is in line with the picture, where photons cannot resolve the individual collisions any more. Since the soft part of the spectrum behaves like  $\omega/\Gamma_x$ , it shows a genuine non-perturbative feature which cannot be obtained by any power series in  $\Gamma_x$ . For comparison: the dashed lines show the corresponding IQF yields, which agree with the correct rates for the hard part while completely fail and diverge towards the soft end of the spectrum. For non-relativistic sources  $\langle v^2 \rangle \ll 1$  one can ignore the additional  $q$ -dependence (dipole approximation; cf. Fig. 1) and the entire spectrum is determined by one macroscopic scale, the relaxation rate  $\Gamma_x$ . This scale provides a quenching factor

$$C_0(\omega) = \frac{\omega^2}{\omega^2 + \Gamma_x^2} \quad (2)$$

by which the IQF results have to be corrected in order to account for the finite collision time effects in dense matter.

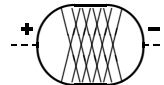
The diffusion result represents a re-summation of the microscopic Langevin multiple collision picture and altogether only macroscopic scales are relevant for the form of the spectrum and not the details of the microscopic collisions. Note also that the classical result fulfill the classical version ( $\hbar \rightarrow 0$ ) of the sum rules discussed in refs. <sup>17,13</sup>.

## 2 Radiation on the Quantum level

We have seen that at the classical level the problem of radiation from dense matter can be solved quite naturally and completely at least for simple examples, and Figs. 1 display the main physics. They show, that the *damping* of the particles due to scattering is an important feature, which in particular has to be included right from the onset. This does not only assure results

that no longer diverge, but also provides a systematic and convergent scheme. On the *quantum level* such problems require techniques beyond the standard repertoire of perturbation theory or the quasi-particle approximation.

In terms of nonequilibrium diagrammatic technique in Keldysh notation, the production or absorption rates are given by photon self-energy diagrams of the type to the right with an in- and out-going photon line (dashed). The hatched loop area denotes all strong interactions of the source. The latter give rise to a whole series of diagrams. As mentioned, for the particles of the source, e.g. the nucleons, one has to re-sum Dyson's equation with the corresponding full complex self-energy in order to determine the full Green's functions in dense matter. Once one has these Green's functions together with the interaction vertices at hand, one could in principle calculate the required diagrams. However, both the computational effort to calculate a single diagram and the number of diagrams increase dramatically with the loop order of the diagrams, such that in practice only lowest-order loop diagrams can be considered in the quantum case. In certain limits some diagrams drop out. We could show that in the *classical limit*, which in this case implies the hierarchy  $\omega, |\mathbf{q}|, \Gamma \ll T \ll m$  together with low phase-space occupations for the source, i.e.  $f(x, p) \ll 1$ , only the following set of diagrams survives



In these diagrams the bold lines denote the full nucleon Green's functions which also include the damping width, the black blocks represent the effective nucleon-nucleon interaction in matter, and the full dots the coupling vertex to the photon. Each of these diagrams with  $n$  interaction loop insertions just corresponds to the  $n^{\text{th}}$  term in the corresponding classical Langevin process, where hard scatterings occur at random with a constant *mean collision rate*  $\Gamma$ . These scatterings consecutively change the velocity of a point charge from  $\mathbf{v}_0$  to  $\mathbf{v}_1$  to  $\mathbf{v}_2, \dots$ . In between scatterings the charge moves freely. For such a multiple collision process the space integrated current-current correlation function takes a simple Poisson form

$$\begin{aligned}
 i\Pi^{\mu\nu-+} &\propto \int d^3x_1 d^3x_2 \langle j^\nu(\mathbf{x}_1, t - \frac{\tau}{2}) j^\mu(\mathbf{x}_2, t + \frac{\tau}{2}) \rangle \\
 &= e^2 \langle v^\mu(0) v^\nu(\tau) \rangle = e^2 e^{-|\Gamma\tau|} \sum_{n=0}^{\infty} \frac{|\Gamma\tau|^n}{n!} \langle v_0^\mu v_n^\nu \rangle
 \end{aligned} \tag{4}$$

with  $v = (1, \mathbf{v})$ . Here  $\langle \dots \rangle$  denotes the average over the discrete collision sequence. This form, which one writes down intuitively, agrees with the analytic result of the quantum correlation diagrams (3) in the limit  $n \ll 1$  and  $\Gamma \ll T$ . Fourier transformed it determines the spectrum in completely regular terms (void of any infra-red singularities), where each term describes the interference of the photon being emitted at a certain time or  $n$  collisions later. In special cases where velocity fluctuations are degraded by a constant fraction  $\alpha$  in each collision, such that  $\langle \mathbf{v}_0 \cdot \mathbf{v}_n \rangle = \alpha^n \langle \mathbf{v}_0 \cdot \mathbf{v}_0 \rangle$ , one can re-sum the whole series in Eq. (4) and thus recover the relaxation result with  $2\Gamma_x \langle \mathbf{v}^2 \rangle = \Gamma \langle (\mathbf{v}_0 - \mathbf{v}_1)^2 \rangle$  at least for  $\mathbf{q} = 0$  and the corresponding quenching factor (2). Thus the classical multiple collision example provides a quite intuitive picture about such diagrams. Further details are given in ref. <sup>13</sup>.

The above example shows that we have to deal with particle transport that explicitly takes account of the particle mass-width in order to properly describe soft radiation from the system.

### 3 The $\rho$ -meson in dense matter

Another example we like to discuss concerns properties of the  $\rho$ -meson and their consequences for the  $\rho$ -decay into di-leptons are discussed. In terms of the nonequilibrium diagrammatic technique, the exact production rate of di-leptons is given by the following formula

$$\begin{aligned}
 \frac{dn^{e^+e^-}}{dt dm} &= \text{Diagram} \\
 &= f_\rho(m, \mathbf{p}, \mathbf{x}, t) A_\rho(m, \mathbf{p}, \mathbf{x}, t) 2m \Gamma^\rho e^+e^-(m). \quad (5)
 \end{aligned}$$

Here  $\Gamma^\rho e^+e^-(m) \propto 1/m^3$  is the mass-dependent electromagnetic decay rate of the  $\rho$  into the di-lepton pair of invariant mass  $m$ . The phase-space distribution  $f_\rho(m, \mathbf{p}, \mathbf{x}, t)$  and the spectral function  $A_\rho(m, \mathbf{p}, \mathbf{x}, t)$  define the properties of the  $\rho$ -meson at space-time point  $\mathbf{x}, t$ . Both quantities are in principle to be determined dynamically by an appropriate transport model. However till to-date the spectral functions are not treated dynamically in most of the present transport models. Rather one employs on-shell  $\delta$ -functions for all stable particles and spectral functions fixed to the vacuum shape for resonances.

As an illustration, the model case is discussed, where the  $\rho$ -meson just strongly couples to two channels, i.e. the  $\pi^+\pi^-$  and  $\pi N \leftrightarrow \rho N$  channels, the latter being relevant at finite nuclear densities. The latter component is

representative for all channels contributing to the so-called *direct*  $\rho$  in transport codes. For a first orientation the equilibrium properties<sup>a</sup> are discussed in simple analytical terms with the aim to discuss the consequences for the implementation of such resonance processes into dynamical transport simulation codes.

Both considered processes add to the total width of the  $\rho$ -meson

$$\Gamma_{\text{tot}}(m, \mathbf{p}) = \Gamma_{\rho \rightarrow \pi^+ \pi^-}(m, \mathbf{p}) + \Gamma_{\rho \rightarrow \pi N N^{-1}}(m, \mathbf{p}), \quad (6)$$

and the equilibrium spectral function then results from the cuts of the two diagrams

$$A_\rho(m, \mathbf{p}) = \underbrace{\text{Diagram 1} + \text{Diagram 2}}_{\frac{2m\Gamma_{\rho \pi^+ \pi^-} + 2m\Gamma_{\rho \pi N N^{-1}}}{(m^2 - m_\rho^2 - \text{Re}\Sigma^R)^2 + m^2\Gamma_{\text{tot}}^2}}. \quad (7)$$

In principle, both diagrams have to be calculated in terms of fully self-consistent propagators, i.e. with corresponding widths for all particles involved. This formidable task has not been done yet. Using micro-reversibility and the properties of thermal distributions, the two terms in Eq. (7) contributing to the dilepton yield (5), can indeed approximately be reformulated as the thermal average of a  $\pi^+ \pi^- \rightarrow \rho \rightarrow e^+ e^-$ -annihilation process and a  $\pi N \rightarrow \rho N \rightarrow e^+ e^- N$ -scattering process, i.e.

$$\frac{dn^{e^+e^-}}{dm dt} \propto \langle f_{\pi^+} f_{\pi^-} v_{\pi\pi} \sigma(\pi^+ \pi^- \rightarrow \rho \rightarrow e^+ e^-) + f_\pi f_N v_{\pi N} \sigma(\pi N \rightarrow \rho N \rightarrow e^+ e^- N) \rangle_T, \quad (8)$$

where  $f_\pi$  and  $f_N$  are corresponding particle occupations and  $v_{\pi\pi}$  and  $v_{\pi N}$  are relative velocities. However, the important fact to be noticed is that in order to preserve unitarity the corresponding cross sections are no longer the free ones, as given by the vacuum decay width in the denominator, but rather involve the *medium dependent total width* (6). This illustrates in simple terms that rates of broad resonances can no longer simply be added in a perturbative way.

<sup>a</sup>Far more sophisticated and in parts unitary consistent equilibrium calculations have already been presented in the literature<sup>18,19,20,21,22</sup>. It is not the point to compete with them at this place.

Di-lepton rates from thermal  $\rho$ -mesons ( $T = 110$  MeV)

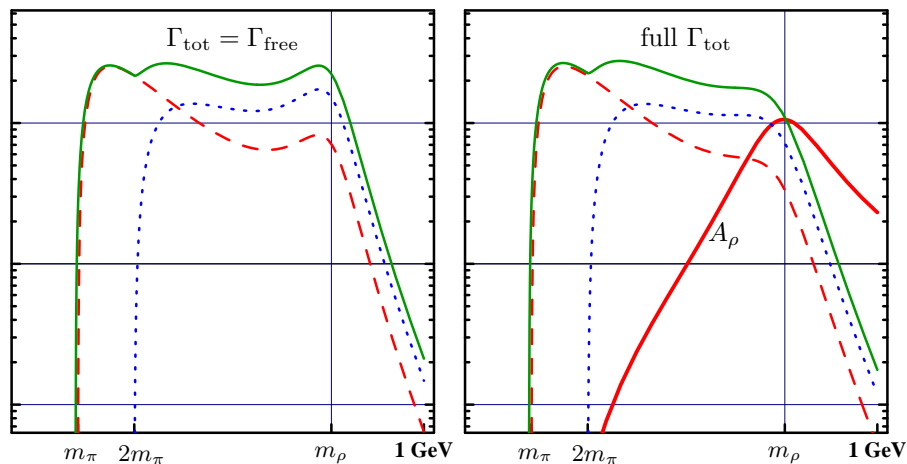


Figure 2:  $e^+e^-$  rates (arb. units) as a function of the invariant pair mass  $m$  at  $T = 110$  MeV from  $\pi^+\pi^-$  annihilation (dotted line) and direct  $\rho$ -meson contribution (dashed line), the full line gives the sum of both contributions. Left part: using the free cross section recipe, i.e. with  $\Gamma_{\text{tot}} = \Gamma_{\rho\pi^+\pi^-}$ ; right part: the correct partial rates (7).  $A_\rho$  is given by the thick line. The calculations are done with  $\Gamma_{\rho\leftrightarrow\pi\pi}(m_\rho) = 150$  MeV and  $\Gamma_{\rho\leftrightarrow\pi NN-1}(m_\rho) = 70$  MeV.

Since it concerns a coupled channel problem, there is a cross talk between the different channels to the extent that the common resonance propagator attains the total width arising from all partial widths feeding and depopulating the resonance. While a perturbative treatment with free cross sections in Eq. (8) would enhance the yield at resonance mass,  $m = m_\rho$ , if a channel is added, cf. Fig. 2 left part, the correct treatment (7) even inverts the trend and indeed depletes the yield at resonance mass, right part in Fig. 2. Furthermore, one sees that only the total yield involves the spectral function, while any partial cross section refers to that partial term with the corresponding partial width in the numerator! Unfortunately so far all these facts have been ignored or even overlooked in the present transport treatment of broad resonances. Compared to the spectral function both thermal components in Fig. 2 show a significant enhancement on the low mass side and a strong depletion at high masses due to the thermal weight  $f \propto \exp(-p_0/T)$  in the rate (5).

As an example we show an exploratory study of the interacting system of  $\pi$ ,  $\rho$  and  $a_1$ -mesons described by the  $\Phi$ -functional



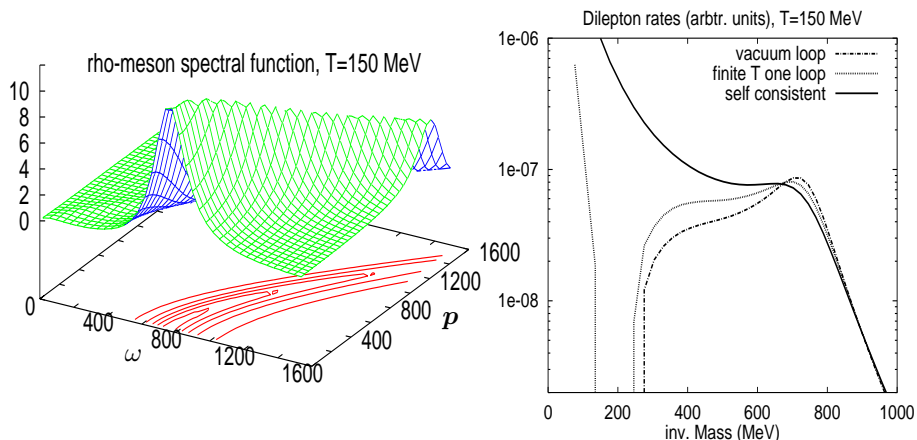


Figure 3: left part: contour plot of the self-consistent spectral function of the  $\rho$ -meson as a function of energy and spatial momentum; right part: thermal di-lepton rate as a function of invariant mass at  $\mathbf{p} = 300 \text{ MeV}/c$

$$\Phi = \begin{array}{c} \pi \\ \circlearrowleft \\ \rho \\ \circlearrowright \\ \pi \end{array} + \begin{array}{c} \pi \\ \circlearrowleft \\ \rho \\ \circlearrowright \\ a_1 \end{array} + \begin{array}{c} \pi \\ \circlearrowleft \\ \pi \\ \circlearrowright \\ \pi \end{array} \quad (9)$$

(cf. section 5 below). The couplings and masses are chosen as to reproduce the known vacuum properties of the  $\rho$  and  $a_1$  meson with nominal masses and widths  $m_\rho = 770 \text{ MeV}$ ,  $m_{a_1} = 1200 \text{ MeV}$ ,  $\Gamma_\rho = 150 \text{ MeV}$ ,  $\Gamma_{a_1} = 400 \text{ MeV}$ . The results of a finite temperature calculation at  $T = 150 \text{ MeV}$  with all self-energy loops resulting from the  $\Phi$ -functional of Eq. (9) computed<sup>23</sup> with self-consistent broad width Green's functions are displayed in Fig. 3 (corrections to the real part of the self-energies were not yet included). The last diagram of  $\Phi$  with the four pion self-coupling has been added in order to supply pion with broad mass-width as they would result from the coupling of pions to nucleons and the  $\Delta$  resonance in nuclear matter environment. As compared to first-order one-loop results which drop to zero below the 2-pion threshold at 280 MeV, the self-consistent results essentially add in strength at the low-mass side of the di-lepton spectrum.

#### 4 Quantum Kinetic Equation

The two above-presented examples unambiguously show that for consistent dynamical treatment of nonequilibrium evolution of soft radiation and broad resonances we need a transport theory that takes due account of mass-widths of constituent particles. A proper frame for such a transport is provided by Kadanoff–Baym equations. We consider the Kadanoff–Baym equations in the

first-order gradient approximation, assuming that time–space evolution of a system is smooth enough to justify this approximation.

First of all, it is helpful to avoid all the imaginary factors inherent in the standard Green function formulation ( $G^{ij}$  with  $i, j \in \{-+\}$ ) and introduce quantities which are real and, in the quasi-homogeneous limit, positive and therefore have a straightforward physical interpretation, much like for the Boltzmann equation. In the Wigner representation we define

$$\begin{aligned} F(X, p) &= A(X, p)f(X, p) = (\mp)\text{i}G^{-+}(X, p), \\ \tilde{F}(X, p) &= A(X, p)[1 \mp f(X, p)] = \text{i}G^{+-}(X, p), \end{aligned} \quad (10)$$

$$A(X, p) \equiv -2\text{Im}G^R(X, p) = \tilde{F} \pm F = \text{i}(G^{+-} - G^{-+}) \quad (11)$$

for the generalized Wigner functions  $F$  and  $\tilde{F}$  with the corresponding *four*-phase-space distribution functions  $f(X, p)$  and Fermi/Bose factors  $[1 \mp f(X, p)]$ , with the spectral function  $A(X, p)$  and the retarded propagator  $G^R$ . Here and below the upper sign corresponds to fermions and the lower one, to bosons. According to relations between Green functions  $G^{ij}$  *only two independent real functions of all the  $G^{ij}$  are required for a complete description*. Likewise the reduced gain and loss rates of the collision integral and the damping rate are defined as

$$\Gamma_{\text{in}}(X, p) = (\mp)\text{i}\Sigma^{-+}(X, p), \quad \Gamma_{\text{out}}(X, p) = \text{i}\Sigma^{+-}(X, p), \quad (12)$$

$$\Gamma(X, p) \equiv -2\text{Im}\Sigma^R(X, p) = \Gamma_{\text{out}}(X, p) \pm \Gamma_{\text{in}}(X, p), \quad (13)$$

where  $\Sigma^{ij}$  are contour components of the self-energy, and  $\Sigma^R$  is the retarded self-energy.

In terms of this notation and within the first-order gradient approximation, the Kadanoff–Baym equations for  $F$  and  $\tilde{F}$  (which result from differences of the corresponding Dyson’s equations with their adjoint ones) take the kinetic form

$$\mathcal{D}F - \{\Gamma_{\text{in}}, \text{Re}G^R\} = C, \quad (14)$$

$$\mathcal{D}\tilde{F} - \{\Gamma_{\text{out}}, \text{Re}G^R\} = \mp C \quad (15)$$

with the drift operator and collision term respectively

$$\mathcal{D} = \left( v_\mu - \frac{\partial \text{Re}\Sigma^R}{\partial p^\mu} \right) \partial_X^\mu + \frac{\partial \text{Re}\Sigma^R}{\partial X^\mu} \frac{\partial}{\partial p_\mu}, \quad v^\mu = (1, \mathbf{p}/m), \quad (16)$$

$$C(X, p) = \Gamma_{\text{in}}(X, p)\tilde{F}(X, p) - \Gamma_{\text{out}}(X, p)F(X, p). \quad (17)$$

Within the same approximation level there are two alternative equations for  $F$  and  $\tilde{F}$

$$MF - \text{Re}G^R\Gamma_{\text{in}} = \frac{1}{4}(\{\Gamma, F\} - \{\Gamma_{\text{in}}, A\}), \quad (18)$$

$$M\tilde{F} - \text{Re}G^R\Gamma_{\text{out}} = \frac{1}{4}(\{\Gamma, \tilde{F}\} - \{\Gamma_{\text{out}}, A\}) \quad (19)$$

with the “mass” function  $M(X, p) = p_0 - \mathbf{p}^2/2m - \text{Re}\Sigma^R(X, p)$ . These two equations result from sums of the corresponding Dyson’s equations with their adjoint ones. Eqs. (18) and (19) can be called the mass-shell equations, since in the quasiparticle limit they provide the on-mass-shell condition  $M = 0$ . Appropriate combinations of the two sets (14)–(15) and (18)–(19) provide us with retarded Green’s function equations, which are simultaneously solved<sup>2,8</sup> by

$$G^R = \frac{1}{M(X, p) + i\Gamma(X, p)/2} \Rightarrow \begin{cases} A = \frac{\Gamma}{M^2 + \Gamma^2/4}, \\ \text{Re}G^R = \frac{M}{M^2 + \Gamma^2/4}. \end{cases} \quad (20)$$

With the solution (20) for  $G^R$  equations (14) and (15) become identical to each other, as well as Eqs. (18) and (19). However, Eqs. (14)–(15) still are not identical to Eqs. (18)–(19), while they were identical before the gradient expansion. Indeed, one can show<sup>24</sup> that Eqs. (14)–(15) differ from Eqs. (18)–(19) in second order gradient terms. This is acceptable within the gradient approximation, however, the still remaining difference in the second-order terms is inconvenient from the practical point of view. Following Botermans and Malfliet<sup>8</sup>, we express  $\Gamma_{\text{in}} = \Gamma f + O(\partial_X)$  and  $\Gamma_{\text{out}} = \Gamma(1 \mp f) + O(\partial_X)$  from the l.h.s. of mass-shell Eqs. (18) and (19), substitute them into the Poisson bracketed terms of Eqs. (14) and (15), and neglect all the resulting second-order gradient terms. The so obtained *quantum four-phase-space kinetic equations for  $F = fA$  and  $\tilde{F} = (1 \mp f)A$*  then read

$$\mathcal{D}(fA) - \{\Gamma f, \text{Re}G^R\} = C, \quad (21)$$

$$\mathcal{D}((1 \mp f)A) - \{\Gamma(1 \mp f), \text{Re}G^R\} = \mp C. \quad (22)$$

These quantum four-phase-space kinetic equations, which are identical to each other in view of retarded relation (20), are at the same time completely identical to the correspondingly substituted mass-shell Eqs. (18) and (19).

The validity of the gradient approximation<sup>24</sup> relies on the overall smallness of the collision term  $C = \{\text{gain} - \text{loss}\}$  rather than on the smallness of the

damping width  $\Gamma$ . Indeed, while fluctuations and correlations are governed by time scales given by  $\Gamma$ , the Kadanoff–Baym equations describe the behavior of the ensemble mean of the occupation in phase-space  $F(X, p)$ . It implies that  $F(X, p)$  varies on space-time scales determined by  $C$ . In cases where  $\Gamma$  is not small enough by itself, the system has to be sufficiently close to equilibrium in order to provide a valid gradient approximation through the smallness of the collision term  $C$ . Both the Kadanoff–Baym (14) and the Botermans–Malfliet choice (21) are, of course, equivalent within the validity range of the first-order gradient approximation. Frequently, however, such equations are used beyond the limits of their validity as ad-hoc equations, and then the different versions may lead to different results. So far we have no physical condition to prefer one of the choices. The procedure, where in all Poisson brackets the  $\Gamma_{\text{in}}$  and  $\Gamma_{\text{out}}$  terms have consistently been replaced by  $f\Gamma$  and  $(1 \mp f)\Gamma$ , respectively, is therefore optional. However, in doing so we gained some advantages. Beside the fact that quantum four-phase-space kinetic equation (21) and the mass-shell equation are then *exactly* equivalent to each other, this set of equations has a particular features with respect to the definition of a nonequilibrium entropy flow in connection with the formulation of an *exact* H-theorem in certain cases. If we omit these substitutions, both these features would become approximate with deviations at the second-order gradient level.

The equations so far presented, mostly with the Kadanoff–Baym choice (14), were the starting point for many derivations of extended Boltzmann and generalized kinetic equations, ever since these equations have been formulated in 1962. Most of those derivations use the equal-time reduction by integrating the four-phase-space equations over energy  $p_0$ , thus reducing the description to three-phase-space information, cf. refs. <sup>4,25,26,27,28,29,30,31,32</sup> and refs. therein. This can only consistently be done in the limit of small width  $\Gamma$  employing some kind of quasi-particle ansatz for the spectral function  $A(X, p)$ . Particular attention has been paid to the treatment of the time-derivative parts in the Poisson brackets, which in the four-phase-space formulation still appear time-local, i.e. Markovian, while they lead to retardation effects in the equal-time reduction. Generalized quasiparticle ansätze were proposed, which essentially improve the quality and consistency of the approximation, providing those extra terms to the naive Boltzmann equation (some times called additional collision term) which are responsible for the correct second-order virial corrections and the appropriate conservation of total energy, cf. <sup>26,29</sup> and refs. therein. However, all these derivations imply some information loss about the differential mass spectrum due to the inherent reduction to a 3-momentum representation of the distribution functions by some specific ansatz. With the aim to treat cases as those displayed in Figs. 2 and 3, where the differential

mass spectrum can be observed by di-lepton spectra, within a self-consistent non-equilibrium approach, one has to treat the differential mass information dynamically, i.e. by means of Eq. (20) avoiding any kind of quasi-particle reductions and work with the full quantum four phase-space kinetic Eq. (21). In the following we discuss the properties of this set of quantum kinetic equations.

## 5 $\Phi$ -derivable approximations

The preceding considerations have shown that one needs a transport scheme adapted to broad resonances. Besides the conservation laws it should comply with requirements of unitarity and detailed balance. A practical suggestion has been given in ref. <sup>7</sup> in terms of cross-sections. However, this picture is tied to the concept of asymptotic states and therefore not well suited for the general case, in particular, if more than one channel feeds into a broad resonance. Therefore, we suggest to revive the so-called  $\Phi$ -derivable scheme, originally proposed by Baym <sup>14</sup> on the basis of the generating functional, or partition sum, given by Luttinger and Ward <sup>33</sup>, and later reformulated in terms of path-integrals <sup>34</sup>. The auxiliary functional  $\Phi$  is given by two-particle irreducible vacuum diagrams. It solely depends on fully re-summed, i.e. self-consistently generated propagators  $iG(x, y) = \langle T_C \hat{\varphi}(x) \hat{\varphi}^\dagger(y) \rangle$ , where  $T_C$  indicates real-time contour ordering. The consistency is provided by the fact that  $\Phi$  is the generating functional for the re-summed self-energy  $\Sigma(x, y)$  via functional variation of  $\Phi$  with respect to any contour ordered propagator  $G(y, x)$ , i.e.

$$-i\Sigma(x, y) = \mp \delta i\Phi / \delta iG(y, x). \quad (23)$$

An extension to include classical fields or condensates into the scheme is presented in ref. <sup>15</sup> In graphical terms, the variation (23) with respect to  $G$  is realized by opening a propagator line in all diagrams of  $\Phi$ . The resulting set of thus opened diagrams must then be that of proper skeleton diagrams of  $\Sigma$  in terms of *full propagators*, i.e. void of any self-energy insertions. As a consequence, the  $\Phi$ -diagrams have to be *two-particle irreducible*, i.e. they cannot be decomposed into two pieces by cutting two propagator lines.

The key property is that truncating the auxiliary functional  $\Phi$  to a limited subset of diagrams leads to a self-consistent, i.e closed, approximation scheme. Thereby the approximate forms of  $\Phi$  define *effective* theories, where  $\Phi^{(\text{appr.})}$  serves as a generating functional for the approximate self-energies  $\Sigma^{(\text{appr.})}(x, y)$  through relation (23), which then enter as driving terms for the Dyson's equations of the different species in the system. As Baym <sup>14</sup> has shown, such a  $\Phi$ -derivable approximation is conserving as related to global symmetries of the original theory. We explicitly cite the forms of the conserved Noether current

and of the energy–momentum tensor, cf. ref. <sup>15</sup>,

$$j^\mu(X) = \frac{e}{2} \int \frac{d^4p}{(2\pi)^4} v^\mu \left( F(X, p) \mp \tilde{F}(X, p) \right), \quad (24)$$

$$\Theta^{\mu\nu}(X) = \frac{1}{2} \int \frac{d^4p}{(2\pi)^4} v^\mu p^\nu \left( F(X, p) \mp \tilde{F}(X, p) \right) + g^{\mu\nu} (\mathcal{E}^{\text{int}} - \mathcal{E}^{\text{pot}}), \quad (25)$$

where

$$\mathcal{E}^{\text{int}}(X) = \left\langle -\hat{\mathcal{L}}^{\text{int}}(X) \right\rangle = - \left. \frac{\delta\Phi}{\delta\lambda(X)} \right|_{\lambda=1}$$

is the density of interaction energy ( $\lambda(X)$  locally scales the coupling strength of vertices, cf. ref. <sup>15</sup>) and the density of potential energy  $\mathcal{E}^{\text{pot}}$  takes the following simple form within the first-order gradient approximation

$$\mathcal{E}^{\text{pot}}(X) = \frac{1}{2} \int \frac{d^4p}{(2\pi)^4} \left[ \text{Re}\Sigma^R \left( F \mp \tilde{F} \right) + \text{Re}G^R \left( \Gamma_{\text{in}} \mp \Gamma_{\text{out}} \right) \right].$$

The first term of  $\mathcal{E}^{\text{pot}}$  complies with quasi-particle expectations, namely mean potential times density, the second term displays the role of fluctuations  $I = \Gamma_{\text{in}} \mp \Gamma_{\text{out}}$  in the potential energy density. This fluctuation term precisely arises from the Poisson bracket term in the kinetic Eq. (21) which induces a back-flow. It restores the Noether expressions (24) and (25) as being indeed the exactly conserved quantities. In this compensation we see the essential role of the fluctuation term in the quantum four-phase-space kinetic equation. Dropping or approximating this term would spoil the conservation laws. Before the gradient expansion, quantities (24) and (25) are *exact* integrals of equations of motion. While after the gradient expansion, they comply with the quantum four-phase-space kinetic equation (21) up to the first-order gradient terms.

At the same time the  $\Phi$ -derivable scheme provides thermodynamical consistency. The latter automatically implies correct detailed balance relations between the various transport processes. For multicomponent systems it leads to a *actio = reactio* principle. This implies that the properties of one species are not changed by the interaction with other species without affecting the properties of the latter ones, too. Some thermodynamic examples have been considered recently, e.g., for the interacting  $\pi N\Delta$  system <sup>12</sup> and for a relativistic QED plasma <sup>35</sup>.

## 6 Collision Term

To further discuss the transport treatment we need an explicit form of the collision term (16), which is provided from the  $\Phi$  functional in the  $-+$  matrix

notation via the variation rules (23) as

$$C(X, p) = \frac{\delta i\Phi}{\delta \tilde{F}(X, p)} \tilde{F}(X, p) - \frac{\delta i\Phi}{\delta F(X, p)} F(X, p). \quad (26)$$

Here we assumed  $\Phi$  be transformed into the Wigner representation and all  $\mp iG^{-+}$  and  $iG^{+-}$  to be replaced by the Wigner-densities  $F$  and  $\tilde{F}$ . Thus, the structure of the collision term can be inferred from the structure of the diagrams contributing to the functional  $\Phi$ . To this end, in close analogy to the consideration of ref. <sup>13</sup>, we discuss various decompositions of the  $\Phi$ -functional, from which the in- and out-rates are derived. For the sake of physical transparency, we confine our treatment to the *local* case, where in the Wigner representation all the Green functions are taken at the same space-time coordinate  $X$  and all non-localities, i.e. derivative corrections, are disregarded. Derivative corrections give rise to memory effects in the collision term, which will be analyzed separately for the specific case of the triangle diagram.

Consider a given closed diagram of  $\Phi$ , at this level specified by a certain number  $n_\lambda$  of vertices and a certain contraction pattern. This fixes the topology of such a contour diagram. It leads to  $2^{n_\lambda}$  different diagrams in the  $-+$  notation from the summation over all  $-+$  signs attached to each vertex. Any  $-+$  notation diagram of  $\Phi$ , which contains vertices of either sign, can be decomposed into two pieces in such a way that each of the two sub-pieces contains vertices of only one type of sign<sup>b</sup>

$$\begin{aligned} i\Phi_{\alpha\beta} &= \left( \alpha \left| \begin{array}{c} \text{---} \\ \text{---} \\ \text{---} \\ \text{---} \\ \text{---} \\ \text{---} \end{array} \right| \beta \right) = \left( \alpha \left| F_1 \dots \tilde{F}'_1 \dots \right| \beta \right) \quad (27) \\ &\Rightarrow \int \frac{d^4 p_1}{(2\pi)^4} \dots \frac{d^4 p'_1}{(2\pi)^4} \dots (2\pi)^4 \delta^4 \left( \sum_i p_i - \sum_i p'_i \right) V_\alpha^* F_1 \dots \tilde{F}'_1 \dots V_\beta \end{aligned}$$

with  $F_1 \dots F_m \tilde{F}'_1 \dots \tilde{F}'_m$  linking the two amplitudes. The  $V_\alpha^*(X; p_1, \dots, p'_1, \dots)$  and  $V_\beta(X; p_1, \dots, p'_1, \dots)$  amplitudes represent multi-point vertex functions of only one sign for the vertices, i.e. they are either entirely time ordered ( $-$  vertices) or entirely anti-time ordered ( $+$  vertices). Here we used the fact that adjoint expressions are complex conjugate to each other. Each such vertex function is determined by normal Feynman diagram rules. Applying the matrix

<sup>b</sup>To construct the decomposition, just deform a given mixed-vertex diagram of  $\Phi$  in such a way that all  $+$  and  $-$  vertices are placed left and respectively right from a vertical division line and then cut along this line.

variation rules (26), we find that the considered  $\Phi$  diagram gives the following contribution to the local part of the collision term (16)

$$C^{\text{loc}}(X, p) \Rightarrow \frac{1}{2} \int \frac{d^4 p_1}{(2\pi)^4} \cdots \frac{d^4 p'_1}{(2\pi)^4} \cdots R \left[ \sum_i \delta^4(p_i - p) - \sum_i \delta^4(p'_i - p) \right] \\ \times \left\{ \tilde{F}_1 \cdots F'_1 \cdots - F_1 \cdots \tilde{F}'_1 \cdots \right\} (2\pi)^4 \delta^4 \left( \sum_i p_i - \sum_i p'_i \right). \quad (28)$$

with the partial process rates

$$R(X; p_1, \dots, p'_1, \dots) = \sum_{(\alpha\beta) \in \Phi} \text{Re} \{ V_\alpha^*(X; p_1, \dots, p'_1, \dots) V_\beta(X; p_1, \dots, p'_1, \dots) \}. \quad (29)$$

The restriction to the real part arises, since with  $(\alpha|\beta)$  also the adjoint  $(\beta|\alpha)$  diagram contributes to this collision term. However these rates are not necessarily positive. In this point, the generalized scheme differs from the conventional Boltzmann kinetics.

An important example of approximate  $\Phi$  which we extensively use below is

$$i\Phi = \frac{1}{2} \text{diagram}_1 + \frac{1}{4} \text{diagram}_2 + \frac{1}{6} \text{diagram}_3 \quad (30)$$

where logarithmic factors due to the special features of the  $\Phi$ -diagrammatic technique are written out explicitly, cf. ref. <sup>24</sup>. In this example we assume a system of fermions interacting via a two-body potential  $V = V_0 \delta(x - y)$ , and, for the sake of simplicity, disregard its spin structure. The  $\Phi$  functional of Eq. (30) results in the following local collision term

$$C^{\text{loc}} = d^2 \int \frac{d^4 p_1}{(2\pi)^4} \frac{d^4 p_2}{(2\pi)^4} \frac{d^4 p_3}{(2\pi)^4} \left( \left| \text{diagram}_1 \right|^2 + \left| \text{diagram}_2 \right|^2 - \left| \text{diagram}_3 \right|^2 \right) \\ \times \delta^4(p + p_1 - p_2 - p_3) \left( F_2 F_3 \tilde{F} \tilde{F}_1 - \tilde{F}_2 \tilde{F}_3 F F_1 \right), \quad (31)$$

where  $d$  is the spin (and maybe isospin) degeneracy factor. From this example one can see that the positive definiteness of transition rate is not evident.

The first-order gradient corrections to the local collision term (28) are called *memory* corrections. *Only diagrams of third and higher order in the number of vertices give rise to memory effects.* In particular, only the last diagram of Eq. (30) gives rise to the memory correction, which is calculated in ref. <sup>24</sup>.



## 7 Entropy

Compared to exact descriptions, which are time reversible, reduced description schemes in terms of relevant degrees of freedom have access only to some limited information and thus normally lead to irreversibility. In the Green's function formalism presented here the information loss arises from the truncation of the exact Martin–Schwinger hierarchy, where the exact one-particle Green function couples to the two-particle Green functions, cf. refs. <sup>2,8</sup>, which in turn are coupled to the three-particle level, etc. This truncation is achieved by the standard Wick decomposition, where all observables are expressed through one-particle propagators and therefore higher-order correlations are dropped. This step provides the Dyson's equation and the corresponding loss of information is expected to lead to a growth of entropy with time.

We start with general manipulations which lead us to definition of the kinetic entropy flow. We multiply Eq. (21) by  $-\ln(F/A)$ , Eq. (22) by  $(\mp)\ln(\tilde{F}/A)$ , take their sum, integrate it over  $d^4p/(2\pi)^4$ , and finally sum the result over internal degrees of freedom like spin (Tr). Then we arrive at the following relation

$$\partial_\mu s_{\text{loc}}^\mu(X) = \text{Tr} \int \frac{d^4p}{(2\pi)^4} \ln \frac{\tilde{F}_a}{F} C(X, p), \quad (32)$$

where the quantity

$$s_{\text{loc}}^\mu = \text{Tr} \int \frac{d^4p}{(2\pi)^4} \frac{A^2\Gamma}{2} \left[ \left( v^\mu - \frac{\partial \text{Re}\Sigma^R}{\partial p_\mu} \right) - M\Gamma^{-1} \frac{\partial \Gamma}{\partial p_\mu} \right] \sigma(X, p) \quad (33)$$

(where  $\sigma(X, p) = \mp[1 \mp f] \ln[1 \mp f] - f \ln f$ ) obtained from the l.h.s. of the kinetic equation is interpreted as the local (Markovian) part of the entropy flow. Indeed, the  $s_{\text{loc}}^0$  has proper thermodynamic and quasiparticle limits <sup>24</sup>. However, to be sure that this is indeed the entropy flow we must prove the H-theorem for this quantity.

First, let us consider the case, when memory corrections to the collision term are negligible. Then we can make use of the form (28) of the local collision term. Thus, we arrive at the relation

$$\begin{aligned} & \text{Tr} \int \frac{d^4p}{(2\pi)^4} \ln \frac{\tilde{F}}{F} C_{\text{loc}}(X, p) \Rightarrow \text{Tr} \frac{1}{2} \int \frac{d^4p_1}{(2\pi)^4} \dots \frac{d^4p'_1}{(2\pi)^4} \dots R \\ & \times \left\{ F_1 \dots \tilde{F}'_1 \dots - \tilde{F}_1 \dots F'_1 \dots \right\} \ln \frac{F_1 \dots \tilde{F}'_1 \dots}{\tilde{F}_1 \dots F'_1 \dots} (2\pi)^4 \delta^4 \left( \sum_i p_i - \sum_i p'_i \right). \quad (34) \end{aligned}$$

In case all rates  $R$  are non-negative, i.e.  $R \geq 0$ , this expression is non-negative, since  $(x - y) \ln(x/y) \geq 0$  for any positive  $x$  and  $y$ . In particular,  $R \geq 0$  takes place for all  $\Phi$ -functionals up to two vertices. Then the divergence of  $s_{\text{loc}}^\mu$  is non-negative

$$\partial_\mu s_{\text{loc}}^\mu(X) \geq 0, \quad (35)$$

which proves the  $H$ -theorem in this case with (33) as the nonequilibrium entropy flow. However, as has been mentioned above, we are unable to show that  $R$  always takes non-negative values for all  $\Phi$ -functionals.

If memory corrections are essential, the situation is even more involved. Let us consider this situation again at the example of the  $\Phi$  approximation given by Eq. (30). We assume that the fermion–fermion potential interaction is such that the corresponding transition rate of the corresponding local collision term (31) is always non-negative, so that the  $H$ -theorem takes place in the local approximation, i.e. when we keep only  $C^{\text{loc}}$ . Here we will schematically describe calculations of ref. <sup>24</sup> which, to our opinion, illustrate a general strategy for the derivation of memory correction to the entropy, provided the  $H$ -theorem holds for the local part.

Now Eq. (32) takes the form

$$\partial_\mu s_{\text{loc}}^\mu(X) = \text{Tr} \int \frac{d^4 p}{(2\pi)^4} \ln \frac{\tilde{F}}{F} C^{\text{loc}} + \text{Tr} \int \frac{d^4 p}{(2\pi)^4} \ln \frac{\tilde{F}}{F} C^{\text{mem}}, \quad (36)$$

where  $s_{\text{loc}}^\mu$  is still the Markovian entropy flow defined by Eq. (33). Our aim here is to present the last term on the r.h.s. of Eq. (36) in the form of full  $x$ -derivative

$$\text{Tr} \int \frac{d^4 p}{(2\pi)^4} \ln \frac{\tilde{F}}{F} C^{\text{mem}} = -\partial_\mu s_{\text{mem}}^\mu(X) + \delta c_{\text{mem}}(X) \quad (37)$$

of some function  $s_{\text{mem}}^\mu(X)$ , which we then interpret as a non-Markovian correction to the entropy flow of Eq. (33) plus a correction ( $\delta c_{\text{mem}}$ ). For the memory induced by the triangle diagram of Eq.(30) detailed calculations of ref. <sup>24</sup> show that the smallness of the  $\delta c_{\text{mem}}$ , originating from small space–time gradients and small deviation from equilibrium, allows us to neglect this term as compared to the first term in r.h.s. of Eq. (37). Thus, we obtain

$$\partial_\mu (s_{\text{loc}}^\mu + s_{\text{mem}}^\mu) \simeq \text{Tr} \int \frac{d^4 p}{(2\pi)^4} \ln \frac{\tilde{F}}{F} C^{\text{loc}} \geq 0, \quad (38)$$

which is the  $H$ -theorem for the non-Markovian kinetic equation under consideration with  $s_{\text{loc}}^\mu + s_{\text{mem}}^\mu$  as the proper entropy flow. The r.h.s. of Eq. (38) is

non-negative provided the corresponding transition rate in the local collision term of Eq. (31) is non-negative.

The explicit form of  $s_{\text{mem}}^\mu$  is very complicated, see ref. <sup>24</sup>. In equilibrium at low temperatures we get  $s_{\text{mem}}^0 \sim T^3 \ln T$  which gives the leading correction to the standard Fermi-liquid entropy. This is the famous correction <sup>36,37</sup> to the specific heat of liquid  ${}^3\text{He}$ . Since this correction is quite comparable (numerically) to the leading term in the specific heat ( $\sim T$ ), one may claim that *liquid  ${}^3\text{He}$  is a liquid with quite strong memory effects from the point of view of kinetics.*

## 8 Summary

A number of problems arising in different dynamical systems, e.g. in heavy-ion collisions, require an explicit treatment of dynamical evolution of particles with finite mass-width. This was demonstrated for the example of bremsstrahlung from a nuclear source, where the soft part of the spectrum can be reproduced only provided the mass-widths of nucleons in the source are taken explicitly into account. In this case the mass-width arises due to collisional broadening of nucleons. Another example considered concerns propagation of broad resonances (like  $\rho$ -meson) in the medium. Decays of  $\rho$ -mesons are an important source of di-leptons radiated by excited nuclear matter. As shown, a consistent description of the invariant-mass spectrum of radiated di-leptons can be only achieved if one accounts for the in-medium modification of the  $\rho$ -meson width (more precisely, its spectral function).

We have argued that the Kadanoff–Baym equation within the first-order gradient approximation, slightly modified to make the set of Dyson’s equations *exactly* consistent (rather than up to the second-order gradient terms), provide a proper frame for a quantum four-phase-space kinetic description that applies also to systems of unstable particles. This quantum four-phase-space kinetic equation proves to be charge and energy–momentum conserving and thermodynamically consistent, provided it is based on a  $\Phi$ -derivable approximation. The  $\Phi$  functional also gives rise to a very natural representation of the collision term. Various self-consistent approximations are known since long time which do not explicitly use the  $\Phi$ -derivable concept like self-consistent Born and T-matrix approximations. The advantage the  $\Phi$  functional method consists in offering a regular way of constructing various self-consistent approximations.

We have also addressed the question whether a closed nonequilibrium system approaches the thermodynamic equilibrium during its evolution. We obtained a definite expression for a local (Markovian) entropy flow and were able to explicitly demonstrate the  $H$ -theorem for some of the common choices of  $\Phi$

approximations. This expression holds beyond the quasiparticle picture and thus generalizes the well-known Boltzmann kinetic entropy. Memory effects in the quantum four-phase-space kinetics were discussed and a general strategy to deduce memory corrections to the entropy was outlined.

**Acknowledgment:** We are grateful to G. Baym, G.E. Brown, P. Danielewicz, H. Feldmeier, B. Friman, E.E. Kolomeitsev and P.C. Martin for fruitful discussions. Two of us (Y.B.I. and D.N.V.) highly appreciate the hospitality and support rendered to us at Gesellschaft für Schwerionenforschung and by the Niels Bohr Institute. This work has been supported in part by BMBF (WTZ project RUS-656-96). Y.B.I. acknowledges partial support of Alexander-von-Humboldt Foundation.

## References

1. J. Schwinger, *J. Math. Phys.* **2**, 407 (1961).
2. L.P. Kadanoff and G. Baym, *Quantum Statistical Mechanics* (Benjamin, 1962).
3. L.P. Keldysh, *ZhETF* **47**, 1515 (1964) [*Sov. Phys. JETP* **20**, 1018 (1965)].
4. B. Bezzerides and D.F. DuBois, *Ann. Phys. (N.Y.)* **70**, 10 (1972).
5. P. Danielewicz, *Ann. Phys. (N.Y.)* **152**, 239 (1984).
6. N.P. Landsmann, *Phys. Rev. Lett.*, **60** 1990 (1988); *Ann. Phys.* **186**, 141 (1988).
7. P. Danielewicz and G. Bertsch, *Nucl. Phys. A* **533**, 712 (1991).
8. W. Botermans and R. Malfliet, *Phys. Rep.* **198**, 115 (1990).
9. M. Herrmann, B.L. Friman, and W. Nörenberg, *Nucl. Phys. A* **560**, 411 (1993).
10. P.A. Henning, *Phys. Rep.* **253**, 235 (1995); *Nucl. Phys. A* **582**, 633 (1995).
11. P.A. Henning and E. Quack, *Phys. Rev. Lett.* **75**, 2811 (1995); *Phys. Rev. D* **54**, 3125 (1996).
12. W. Weinhold, *Diploma thesis* GSI 1995; W. Weinhold, B.L. Friman, and W. Nörenberg, *Acta Phys. Pol.* **27**, 3249 (1996); *Phys. Lett. B* **433**, 236 (1998).
13. J. Knoll and D.N. Voskresensky, *Ann. Phys.* **249**, 532 (1996); *Phys. Lett. B* **351**, 43 (1995).
14. G. Baym, *Phys. Rev.* **127**, 1391 (1962).
15. Yu.B. Ivanov, J. Knoll, and D.N. Voskresensky, *Nucl. Phys. A* **657**, 413 (1999).

16. L. D. Landau and I. Pomeranchuk, *Dokl. Akad. Nauk SSSR* **92**, 553, 735 (1953); see also *Collected Papers of Landau*, ed. Ter Haar (Gordon & Breach, 1965) papers 75 - 77; A. B. Migdal, *Phys. Rev.* **103**, 1811 (1956); *Sov. Phys. JETP* **5**, 527 (1957).
17. J. Knoll and C. Guet, *Nucl. Phys. A* **494**, 334 (1989); M. Durand and J. Knoll, *Nucl. Phys. A* **496**, 539 (1989).
18. R. Rapp, G. Chanfray, and J. Wambach, *Nucl. Phys. A* **617**, 472 (1997).
19. S. Leupold, U. Mosel, *Phys. Rev. C* **58**, 2939 (1998).
20. F. Klingl, N. Kaiser, and W. Weise, *Nucl. Phys. A* **624**, 527 (1997).
21. B.L. Friman and H.-J. Pirner, *Nucl. Phys. A* **617**, 496 (1997)
22. B. Friman, M. Lutz and G. Wolf, GSI-Preprint-98-63, nucl-th/9811040.
23. H. van Hees and J. Knoll, to be published.
24. Yu.B. Ivanov, J. Knoll and D.N. Voskresensky, nucl-th/9905028, *Nucl. Phys. A*, in print.
25. P. Lipavsky, V. Spicka and B. Velicky, *Phys. Rev. D* **34**, 6933 (1986).
26. V. Spicka and P. Lipavsky, *Phys. Rev. Lett.* **73**, 3439 (1994); *Phys. Rev. B* **52**, 14615 (1995).
27. W.D. Kraeft, D. Kremp, W. Ebeling and G. Röpke, *Quantum Statistics of Charged Particle Systems* (Akademie-Verlag, Berlin, 1986).
28. M. Bonitz, *Quantum Kinetic Theory* (Teubner, Stuttgart/Leipzig, 1998).
29. Th. Bornath, D. Kremp, W. D. Kraeft, and M. Schlanges, *Phys. Rev. E* **54**, 3274 (1996).
30. M. Schönhofen, M. Cubero, B. Friman, W. Nörenberg and Gy. Wolf, *Nucl. Phys. A* **572**, 112 (1994).
31. S. Jeon and L.G. Yaffe, *Phys. Rev. D* **53**, 5799 (1996).
32. D.N. Voskresensky, D. Blaschke, G. Röpke and H. Schulz, *Int. Mod. Phys. J. E* **4**, 1 (1995).
33. J. M. Luttinger and J. C. Ward, *Phys. Rev.* **118**, 1417 (1960).
34. J.M. Cornwall, R. Jackiw and E. Tomboulis, *Phys. Rev. D* **10**, 2428 (1974).
35. B. Vanderheyden and G. Baym, *J. Stat. Phys.* **93**, 843 (1998).
36. G. Baym and C. Pethick, *Landau Fermi-Liquid Theory* (John Wiley and Sons, INC, N.Y., 1991).
37. G.M. Carneiro and C. J. Pethick, *Phys. Rev. B* **11**, 1106 (1975).